

Local Orientation Variations in YBCO Films on Technical Substrates - A Combined SEM and EBSD Study

Patrick Pahlke, Max Sieger, Paul Chekhanin, Werner Skrotzki, Jens Hänisch,
Alexander Usoskin, Jan Strömer, Ludwig Schultz, and Ruben Hühne

Abstract—Scanning electron microscope imaging and electron backscatter diffraction are applied to 400 nm thick YBCO films grown on Ni-9at.%W and ABAD-YSZ tape. On Ni-9at.%W tape, the orientation of YBCO strongly varies from grain to grain, which is attributed to the different orientations of the underlying substrate grains with regard to the surface normal. On ABAD-YSZ, the structures causing the orientation variations are observed on a micrometer scale only, which is attributed to the granularity of the template. In contrast to Ni-9at.%W where no preferred misorientation axis is notable within single substrate grains, the misorientation of YBCO on the ABAD-YSZ tape is primarily caused by lattice rotations about the sample normal.

Index Terms—Coated conductors, electron backscatter diffraction (EBSD), orientation, pulsed laser deposition (PLD), YBCO.

I. INTRODUCTION

THE template used for the preparation of $\text{YBa}_2\text{Cu}_3\text{O}_{7-\delta}$ (YBCO) based coated conductors affects the superconducting properties in multiple ways. It is therefore essential to understand how the template influences the structural and crystalline quality of the YBCO film.

The major techniques to achieve a biaxially textured tape are rolling assisted biaxially textured substrates (RABiTS) and ion beam assisted deposition (IBAD) [1]. The RABiTS approach is based on a rolling and annealing treatment of a Ni-based alloy, which leads to a strong recrystallization texture with biaxially aligned grains. In highly alloyed Ni-9at.%W tapes, the Curie point is strongly suppressed compared to tapes with lower

W-content leading to a reduction of AC losses at low temperatures [2], while still showing a 96% fraction of cube texture ($< 10^\circ$ criterion) [3]. In contrast, the IBAD approach is applied to polycrystalline substrates. The textured layer is created by an assisting ion-beam during its deposition, leading to a biaxial alignment of the deposited material. A special form of IBAD is alternating beam assisted deposition (ABAD) to preferentially orient Y_2O_3 -stabilized ZrO_2 (YSZ). Here, deposition zone and ion-beam zone are separated [4].

The goal of this paper is a qualitative comparison of the local structure and the orientation distribution of YBCO deposited on Ni-9at.%W and ABAD-YSZ tapes. The general results presented are also valid for NiW tapes with lower W content, as these show a similar local structure.

II. EXPERIMENTAL

A. Sample Preparation

YBCO was deposited on two kinds of technical tapes: a RABiTS Ni-9at.%W tape with a PLD- Y_2O_3 /YSZ/ CeO_2 buffer layer system and a stainless steel tape with a PLD- CeO_2 buffered ABAD-YSZ layer. The YBCO layer was deposited by pulsed laser deposition (PLD) from a stoichiometric target on both templates arranged side by side in order to guarantee best comparison. A KrF excimer laser ($\lambda = 248 \text{ nm}$, Coherent LPXpro 305) was used to deposit 3000 pulses YBCO at a laser repetition rate of 10 Hz leading to a layer thickness of around 400 nm. During deposition, an oxygen pressure of 0.4 mbar and a temperature of 810 °C were maintained. To achieve optimally doped YBCO, a subsequent oxygenation step in 400 mbar oxygen completed the process.

B. Structural Characterization

The samples were analyzed by taking secondary electron (SE) images with a *JEOL JSM-6510* scanning electron microscope (SEM) at an acceleration voltage of 20 kV.

Electron backscatter diffraction (EBSD) was performed using a *GEMINI LEO 1530* SEM with a *Nordlys* EBSD detector. An acceleration voltage of 20 kV, a 2×2 binning of the EBSD detector screen and a long exposure time of at least 0.4 seconds per EBSD pattern (EBSP) were used to achieve high quality patterns.

The recorded EBSPs were first saved on the hard disk and indexed after the measurements. This procedure has several advantages. First, it conserves CPU resources so that the measurement can be performed faster, reducing contamination and possible errors due to beam or focus drift. Second, the EBSPs can be analyzed in a post-process with different sets of parameters to achieve a high indexing rate. Third, EBSPs can be manually indexed afterwards, which allows to check for wrongly indexed points in the mapping. To avoid beam drift, the setup including an active electron beam was prepared several hours prior to the EBSD measurement.

EBSM mappings were created with the Oxford Instruments *HKL Channel 5* acquisition software using the advanced fit option for smaller random errors. The extrapolation option down to level 6 and the wild spike extrapolation was applied.

An automatic indexing of the recorded EBSPs using the orthorhombic YBCO phase available in the *HKL* database was not satisfying because it often led to wrong solutions. Therefore, a related tetragonal cuprate phase with a slightly higher c/a ratio was used instead. Indexing using the tetragonal YBCO structure, as well as a cubic version of this structure were reported before [5], [6]. By manually indexing a set of EBSPs using the YBCO phase, it was found that the misorientation provided with the tetragonal solution is overrated by about 10%. Therefore, the misorientation values given in this paper are slightly higher than in reality. From misorientation profiles on homogeneous YBCO areas, the random error of the orientation data was estimated to be lower than 0.4° , thus allowing a detailed misorientation analysis. This is in agreement with a previous publication [7], where an even smaller random error was measured using a comparable experimental EBSD setup and the same evaluation software.

III. RESULTS

A. SEM Investigation

The kind of template apparently affects the growth of the YBCO thin film as already visible on the 100- μm scale in SE images, Fig. 1. YBCO grows very homogeneously on the ABAD tape and only a few pores are visible, Fig. 1(a). On the Ni-9at.%W tape the situation is quite different. The legacy of the recrystallized grains of the Ni-9at.%W tape with a typical grain size of 20 μm to 50 μm can be clearly seen. Because the Ni-9at.%W grains are misoriented against each other, the surface of each single grain can be understood as a template with an individual crystallographic miscut towards the substrate normal. Depending on the miscut angle, the YBCO can grow smooth and dense [blue arrows in Fig. 1(b)] or faceted and porous [red arrows in Fig. 1(b)]. The direction and width of the facets are varying from grain to grain. Measurements performed by atomic force microscopy revealed a terrace width of around 400 nm and a step height of around 25 nm for one selected grain. The corresponding inclination angle can be calculated to $\sim 4^\circ$, which is a reasonable value (see Section III-B). This terrace morphology strongly reminds of YBCO grown on inclined substrate deposition (ISD) tapes (see [8], [9]) and is similar to films prepared on vicinal SrTiO_3 substrates but at a different length scale [10]–[12]. In both cases, the inclination is constant over the whole sample.

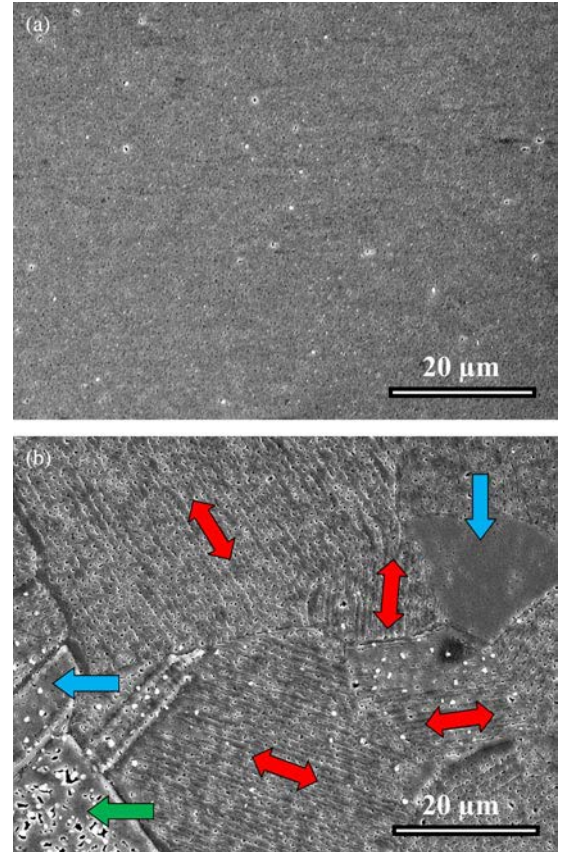


Fig. 1. SE image of YBCO deposited on (a) ABAD-YSZ and (b) Ni-9at.%W tape. The blue arrows are pointing to flat grain surfaces, whereas the green arrow points to a grain with large pores. The red arrows indicate the direction of terraces in the faceted grain surfaces.

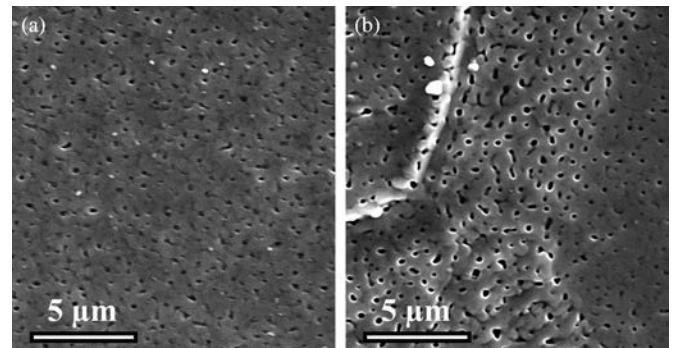


Fig. 2. Higher magnification SE image of YBCO deposited on (a) ABAD-YSZ and (b) Ni-9at.%W tape.

Regions with large pores [green arrow in Fig. 1(b)] and segregations [white particles in Fig. 1(b)] are also found. The density of segregations (most probably CuO_x particles) varies strongly between the single grains. Some grains are totally free while others are densely covered by particles. These segregations appear preferentially on grains with a misorientation larger than 6° with respect to the ideal cube texture. This implies that the ability to form these segregations is strongly correlated to the individual miscut angle of the related substrate grain.

At higher magnification (Fig. 2) the structure of merging YBCO islands (areas between pores, estimated upper grain

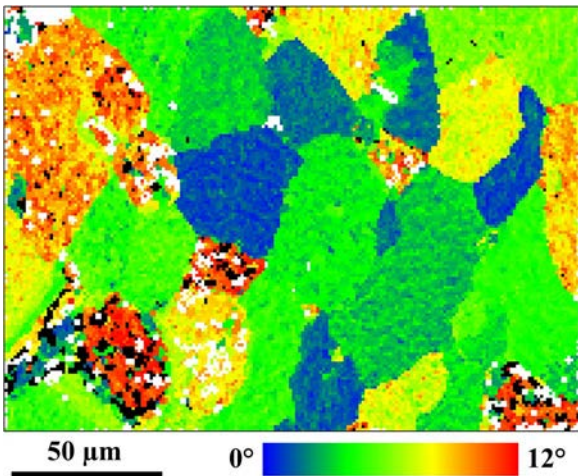


Fig. 3. EBSD mapping (step size 1 μm) of YBCO deposited on Ni-9at.%W tape showing the absolute misorientation from the ideal cube texture. White: nonindexed areas; black: misorientation $> 12^\circ$.

size 0.3 μm –0.8 μm) is visible on both templates. The islands appear rather round on the ABAD tape, whereas they are more elongated on the Ni-9at.%W tape. Additionally, the surface roughness as well as density and size of the pores vary more strongly on the Ni-9at.%W tape.

B. EBSD Investigation—Mappings

In general, YBCO grows epitaxially on the provided templates except on highly misoriented areas such as recrystallization twins [13]. Therefore, the granular structure of the underlying Ni-9at.%W tape is still observable on the 100- μm scale in the EBSD mappings (Fig. 3). The majority of grains are highly cube-oriented with deviations from ideal cube texture of less than 12°. Only a few areas (< 5%) exhibit larger values (black points in Fig. 3). The substructure within a Ni-9at.%W grain demonstrates that the orientation of YBCO growing on a single grain of the template is not constant. This local orientation distribution varies significantly from grain to grain and may be the result of the lattice misfit accommodation as well as the adjustment to the local surface structure. The misorientation within a grain is clearly visible in EBSD mappings with a small step size (Fig. 4).

The situation is different for the ABAD tape. This template is homogeneous and therefore granularity of the YBCO film is not observed on the 100- μm scale. Granularity is first seen in EBSD mappings with a step size below 100 nm (Fig. 5). Only very few sites ($\sim 1\%$) of the YBCO film show a misorientation larger than 5°.

C. EBSD Investigation—Line Scans

The EBSD mappings discussed in the previous section show the misorientation angle with respect to the ideal cube orientation. This information alone is insufficient for determining the rotation axis. To analyze this, the angular deviation of the [100], [010], and [001] YBCO axis from the rolling, transverse and normal direction of the thin film, respectively, needs to be taken

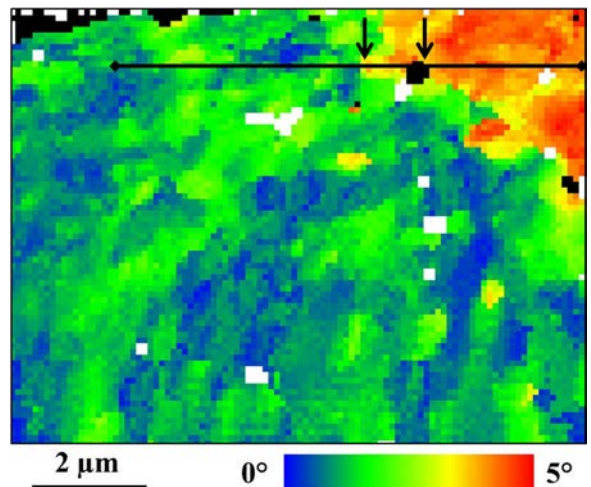


Fig. 4. EBSD mapping (step size 0.1 μm) of YBCO deposited on Ni-9at.%W tape showing the absolute misorientation from the ideal cube texture. White: nonindexed areas; black: misorientation $> 5^\circ$. The black line indicates the position of the line scan, and the arrows point to the location of grain boundaries.

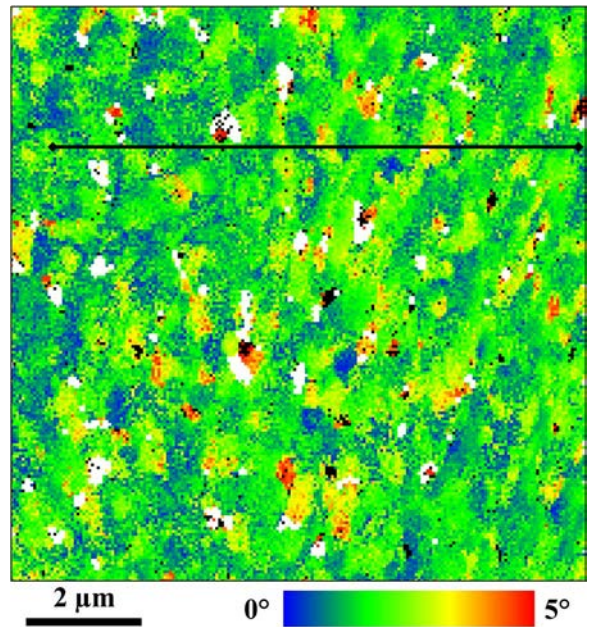


Fig. 5. EBSD mapping (step size 0.05 μm) of YBCO deposited on ABAD-YSZ tape showing the absolute misorientation from the ideal cube texture. White: nonindexed areas; black: misorientation $> 5^\circ$. The black line indicates the position of the line scan.

into account. Instead of showing additional mappings for each of the three symmetry axis, line scans across these images have been taken and combined in angular deviation-distance graphs (Figs. 6 and 7). The positions of the line scans are shown in the EBSD mappings in Figs. 4 and 5.

For the Ni-9at.%W tape, the line scan crosses two grain boundaries (arrows in Fig. 4 and dotted lines in Fig. 6). Along the chosen line scan an internal angular deviation (within one grain) with respect to all three sample axes can be observed. The curves for different sample axes are not always correlated, which means, that the rotation of the YBCO cell does not have

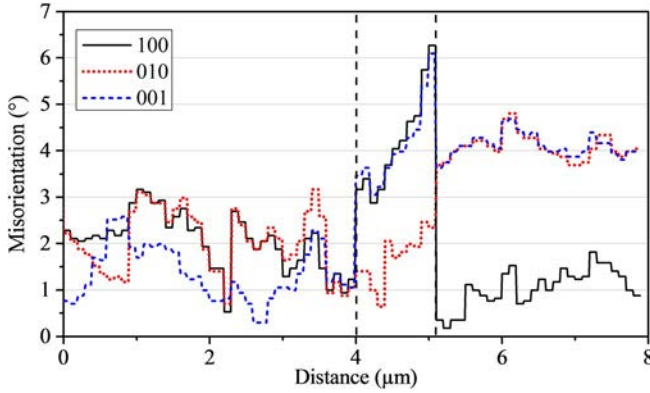


Fig. 6. EBSD line scan across an area of the EBSD mapping Fig. 4 of YBCO deposited on Ni-9at.%W tape (step size $0.1 \mu\text{m}$). The three plotted lines show the angular deviation of the [100]-, [010]-, and [001]-YBCO axis from the rolling, transverse, and normal direction of the thin film, respectively. The location of the grain boundaries is indicated by dotted lines.

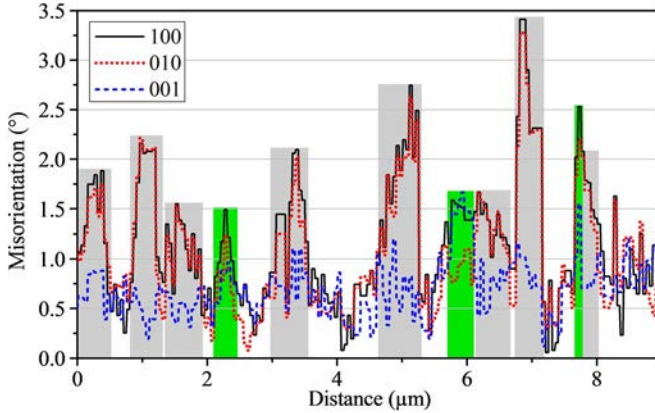


Fig. 7. EBSD line scan across an area of the EBSD mapping Fig. 5 of YBCO deposited on ABAD-YSZ tape (step size $0.05 \mu\text{m}$). The three plotted lines show the angular deviation of the [100]-, [010]-, and [001]-YBCO axis from the rolling, transverse, and normal direction of the thin film, respectively. Take note of the equal-length scale but different misorientation scale compared with Fig. 6. For an explanation of the colored areas, see text.

a preferred axis. However, the internal angular deviations are limited to about 3° .

On the ABAD tape the normal direction of the thin film is found to be an invariant rotation axis (Fig. 7). There is almost no deviation of the [001] YBCO axis from the normal direction (few exceptions marked green in Fig. 7), while the angular deviation of the [100] and [010] YBCO axis from the rolling and transverse direction, respectively, strongly correlate and overlap in most parts (gray areas in Fig. 7). The angular deviation of the [001] YBCO axis from the normal direction is as low as 1° . The high grade of *c*-axis alignment is confirmed by global texture measurements with a peak full width at half maximum (FWHM) of $\sim 1.4^\circ$ for an ω -scan of the YBCO (005) peak. Corresponding measurements on the Ni-9at.%W tape yield a FWHM of $\sim 2.2^\circ$. The angular deviation of the [100] and [010] YBCO axis from the rolling and transverse direction shows typically values of 1° to 3° (Fig. 7). These values appear generally comparable to the internal misorientation distribution on grains of the Ni-9at.%W tape (Fig. 6).

IV. DISCUSSION

The origin of the internal misorientation of YBCO on Ni-9at.%W tapes may be due to different miscut angles of the underlying Ni-9at.%W grain: On grains with low miscut, YBCO finds nearly single crystalline growth conditions and therefore exhibits a sharp texture, whereas on more tilted grains, YBCO grows faceted and porous leading to local rotations of the YBCO unit cell and a broader local orientation distribution.

The YSZ layer of the ABAD tape is textured due to growth selection during the IBAD step [14]. The evolving YSZ grains grow columnar, with a slight in-plane misorientation against each other. From TEM investigations the diameter of the columnar grains is estimated to be between 200 nm and 300 nm . In previous studies, some kind of growth selection was observed in the YBCO layer itself, leading to an increased grain size and sharper texture with increasing film thickness [15]. Therefore, those areas where the sample normal direction appears to be the sole major rotation axis (marked grey in Fig. 7) may be attributed to single or a few merged YBCO grains. This is supported by the SEM investigations (Section III-A.), where it is found that the size of single or a few coalescent grains matches with the structural dimensions in the EBSD mappings (Fig. 5) and the line scans (Fig. 7).

V. CONCLUSION

The SEM and EBSD investigations reveal a microstructure of YBCO being highly influenced by the template material. On Ni-9at.%W tape the YBCO grows on Ni-9at.%W grains with different miscut angles, leading to a diverse microstructure, ranging from dense and flat to porous and faceted areas. This may explain the large variations of the internal misorientation amplitudes from all sample axes. Although locally a correlation between the angular deviations from two sample axes is observed, there does not exist a preferred misorientation axis.

YBCO is growing homogeneously on ABAD templates, and structural features are first observed on the micrometer scale. The major part of the misorientation from the ideal cube orientation is caused by a rotation of the YBCO lattice around the sample normal. The length scale of the misoriented areas matches very well with the grain size of the ABAD template.

ACKNOWLEDGMENT

The authors would like to thank D. Geißler for the inspiring discussions.

REFERENCES

- [1] X. Obradors and T. Puig, "Coated conductors for power applications: Materials challenges," *Supercond. Sci. Technol.*, vol. 27, no. 4, Mar. 2014, Art. no. 044003.
- [2] U. Gaitzsch *et al.*, "Highly alloyed Ni-W substrates for low AC loss applications," *Supercond. Sci. Technol.*, vol. 26, no. 8, pp. 85 024–85 029, Aug. 2013.
- [3] J. Eickemeyer *et al.*, "Textured Ni-9.0% W substrate tapes for YBCO-coated conductors," *Supercond. Sci. Technol.*, vol. 23, no. 8, pp. 85 012–85 017, Aug. 2010.
- [4] A. Usoskin *et al.*, "Processing of long-length YBCO coated conductors based on stainless steel tapes," *IEEE Trans. Appl. Supercond.*, vol. 17, no. 2, pp. 3235–3238, Jun. 2007.

- [5] D. Grossin *et al.*, “EBSD study on YBCO textured bulk samples: Correlation between crystal growth and microtexture,” *Supercond. Sci. Technol.*, vol. 19, no. 2, pp. 190–199, Feb. 2006.
- [6] M. Weigand *et al.*, “Individual grain boundary properties and overall performance of metal-organic deposition coated conductors,” *Phys. Rev. B*, vol. 81, no. 17, May 2010, Art. no. 174537.
- [7] P. Chekhonin, J. Engelmann, C.-G. Oertel, B. Holzapfel, and W. Skrotzki, “Relative angular precision in electron backscatter diffraction: A comparison between cross correlation and Hough transform based analysis,” *Cryst. Res. Technol.*, vol. 49, no. 6, pp. 435–439, Jun. 2014.
- [8] K. K. Upadhyay *et al.*, “Growth and properties of YBCO-coated conductors on biaxially textured MgO films prepared by inclined substrate deposition,” *Supercond. Sci. Technol.*, vol. 18, no. 3, pp. 294–298, Mar. 2005.
- [9] B. Ma *et al.*, “Growth and properties of YBCO-coated conductors fabricated by inclined-substrate deposition,” *IEEE Trans. Appl. Supercond.*, vol. 15, no. 2, pp. 2970–2973, Jun. 2005.
- [10] A. Polyanskii *et al.*, “Magneto-optical imaging and electromagnetic study of $\text{YBa}_2\text{Cu}_3\text{O}_7$ vicinal films of variable thickness,” *Phys. Rev. B*, vol. 72, no. 17, Nov. 2005, Art. no. 174509.
- [11] D. Vassiloyannis and P. M. Pardalos, “Morphological variations on surface topography of $\text{YBa}_2\text{Cu}_3\text{O}_{7-\delta}$ thin films on SrTiO_3 , with respect to the substrate misorientation direction,” *Phys. C, Supercond.*, vol. 468, no. 3, pp. 147–152, Feb. 2008.
- [12] W.-F. Hu *et al.*, “Control of the growth mode of epitaxial *c*-axis $\text{YBa}_2\text{Cu}_3\text{O}_{7-\delta}$ thin films by vicinal (001) SrTiO_3 substrates,” *J. Cryst. Growth*, vol. 231, no. 4, pp. 493–497, Oct. 2001.
- [13] R. Hühne *et al.*, “Application of textured highly alloyed Ni-W tapes for preparing coated conductor architectures,” *Supercond. Sci. Technol.*, vol. 23, no. 3, Mar. 2010, Art. no. 034015.
- [14] J. Dzick, J. Hoffmann, S. Sievers, L. O. Kautschor, and H. C. Freyhardt, “Ion-beam-assisted texturing of YSZ layers,” *Phys. C, Supercond.*, vol. 372, pp. 723–728, Aug. 2002.
- [15] P. Pahlke *et al.*, “Thick High J_c YBCO Films on ABAD-YSZ Templates,” *IEEE Trans. Appl. Supercond.*, vol. 25, no. 3, Jun. 2015, Art. no. 6603804.

Repository KITopen

Dies ist ein Postprint/begutachtetes Manuskript.

Empfohlene Zitierung:

Pahlke, P.; Sieger, M.; Chekhonin, P.; Skrotzki, W.; Hänisch, J.; Usoskin, A.; Stromer, J.; Schultz, L.; Huhne, R.

[Local Orientation Variations in YBCO Films on Technical Substrates-A Combined SEM and EBSD Study.](#)

2016. IEEE transactions on applied superconductivity

[doi:10.5445/IR/1000055365](#)

Zitierung der Originalveröffentlichung:

Pahlke, P.; Sieger, M.; Chekhonin, P.; Skrotzki, W.; Hänisch, J.; Usoskin, A.; Stromer, J.; Schultz, L.; Huhne, R.

[Local Orientation Variations in YBCO Films on Technical Substrates-A Combined SEM and EBSD Study.](#)

2016. IEEE transactions on applied superconductivity, 26 (3), 7420627.

[doi:10.1109/TASC.2016.2535138](#)

Lizenzinformationen: [KITopen-Lizenz](#)